

# Theory of traveling filaments in bistable semiconductor structures

Pavel Rodin\*

*Institut für Theoretische Physik,  
Technische Universität Berlin,  
Hardenbergstrasse 36, D-10623, Berlin, Germany*  
and

*Ioffe Physicotechnical Institute of Russian Academy of Sciences,  
Politechnicheskaya 26, 194021, St. Petersburg, Russia*

(Dated: August 13, 2018)

We present a generic nonlinear model for current filamentation in semiconductor structures with S-shaped current-voltage characteristics. The model accounts for Joule self-heating of a current density filament. It is shown that the self-heating leads to a bifurcation from static to traveling filament. Filaments start to travel when increase of the lattice temperature has negative impact on the cathode-anode transport. Since the impact ionization rate decreases with temperature, this occurs for a wide class of semiconductor systems whose bistability is due to the avalanche impact ionization. We develop an analytical theory of traveling filaments which reveals the mechanism of filament motion, find the condition for bifurcation to traveling filament, and determine the filament velocity.

PACS numbers: 72.20.Ht, 85.30.-z, 05.65.+b

## I. INTRODUCTION

Bistable semiconductor systems with S-shaped current-voltage characteristics exhibit spontaneous formation of current density filaments — high current density domains in the low current density environment.<sup>1,2,3,4,5,6</sup> Current filamentation typically develops due to the spatial long wavelength instability — known as Ridley instability<sup>1</sup> — of the uniform state with negative differential conductance when the device is operated via sufficiently large load resistance,<sup>7,8</sup> Fig. 1. Formation of current filaments potentially leads to thermal destruction of semiconductor structure and thus is an important scenario of semiconductor device failure.<sup>4,6</sup> Current filaments have been studied in bulk semiconductors,<sup>2,5,9,10</sup> thin semiconductor films,<sup>11,12,13,14,15</sup> and layered structures of semiconductor devices.<sup>16,17,18,19,20,21</sup> Over last decade, the focus has been shifted from static filaments to complex spatio-temporal dynamics of current density patterns.<sup>22,23,24,25</sup> Modern experimental techniques based on electron scanning microscopy,<sup>26</sup> detection of infrared radiation,<sup>27</sup> and interferometric mapping<sup>28</sup> provide means for direct observation of current density dynamics during filamentation. In regard to pattern formation and nonlinear phenomena, bistable semiconductors have much in common with other spatially distributed active media such as gas discharge systems, chemical and biological systems.<sup>22,29,30,31,32,33</sup>

Apart from the well understood bifurcation which leads to temporal periodic or chaotic oscillations,<sup>34,35,36,37</sup> static filament may undergo a secondary bifurcation that leads to traveling filament. Lateral movement of filaments along the device has been observed experimentally for different types of semiconductor structures.<sup>27,28,38,39</sup> Remarkably, in all

these structures the S-shaped characteristic is associated with avalanche impact ionization. Since impact ionization coefficients decrease with temperature,<sup>4</sup> the onset of filament motion has been attributed to the self-heating of the filament.<sup>40</sup> the filament is expected to migrate to a colder region as temperature at its initial location increases. When current filamentation is unavoidable, the migration is desirable in applications because the filament motion delocalizes the heating of the semiconductor structure and thus reduces the hazard of thermal destruction.

The purpose of this paper is to describe the mechanism of filament motion, to develop a generic nonlinear model for traveling filament, to find the condition for bifurcation to traveling filament, and to determine the filament velocity. We demonstrate that the transition from static to traveling filament due to the Joule self-heating represents a generic effect which potentially appears in any bistable semiconductor structure provided that transport in the cathode-anode direction is sensitive to temperature.

## II. MODEL OF A BISTABLE SEMICONDUCTOR SYSTEM

For many semiconductors and semiconductor devices current filamentation can be described by a two-component reaction-diffusion model which consists of a partial differential equation for the bistable element and an integro-differential Kirchhoff's equation for the external circuit<sup>7,8,41</sup>

$$\frac{\partial a}{\partial t} = \nabla_{\perp} (D_a(a) \nabla_{\perp} a) + f(a, u), \quad \nabla_{\perp} \equiv \mathbf{e}_x \partial_x + \mathbf{e}_y \partial_y, \quad (1)$$

$$\tau_u \frac{du}{dt} = U_0 - u - R \int_S J(a, u) dx dy, \quad \tau_u \equiv RC. \quad (2)$$

Here the variable  $a(x, y, t)$  characterizes the internal state of the device and the variable  $u(t)$  is the voltage over the device,  $U_0$  is the total applied voltage,  $J$  is the current density,  $R$  is the load resistance connected in series with the device,  $C$  is the effective capacitance of the device and the external circuit, and  $S$  is the device cross-section (Fig. 1). The local kinetic function  $f(a, u)$  and the  $J(a, u)$  dependence contain all information about transport in the cathode-anode (vertical) direction; the diffusion coefficient  $D_a(a)$  characterizes lateral coupling in the spatially extended element. In the bistability range  $u_h < u < u_{th}$  (see Fig. 1) the local kinetic function  $f(a, u)$  has three zeros  $a_{\text{off}}, a_{\text{int}}, a_{\text{on}}$  corresponding to off, intermediate, and on branches of current voltage characteristic. It has one zero outside the bistability range. For the homogeneous state, the local dependence  $a(u)$  is calculated from  $f(a, u) = 0$ , and then inserted into  $J(a, u)$  in order to determine the local current-voltage characteristic  $J(u) \equiv J(a(u), u)$ . Typically  $\partial_u f, \partial_a j, \partial_u j > 0$ . The model (1), (2) belongs to a class of activator-inhibitor models with global inhibition.<sup>25</sup> Variables  $a$  and  $u$  serve as activator and inhibitor, respectively. The time scale of the activator  $a$  is  $\tau_a = \partial_a f^{-1}$ .<sup>7</sup> Specific functional forms  $f(a, u)$ ,  $j(a, u)$ , and  $D_a(a)$  have been derived for various semiconductors and semiconductor structures.<sup>2,7,8,9,10,17,18,20,34,41,42</sup> The physical meaning of  $a$  depends on the particular type of bistable structure:  $a$  corresponds to the bias of the emitter  $p$ - $n$  junction for avalanche transistors,<sup>18</sup> thyristors<sup>20</sup> and thyristorlike structures,<sup>21</sup> interface charge for heterostructure hot electron diode,<sup>34</sup> electron charge stored in the quantum well for bistable double barrier resonant tunneling diode,<sup>41,42</sup> etc.

The two-component model (1), (2) is capable to describe steady filaments<sup>8</sup> as well as temporal oscillation of current density filaments.<sup>34,36,37</sup> However, its solutions do not include traveling filaments.

The self-heating of the filament has an impact on filament dynamics when vertical transport is sensitive to temperature. In terms of Eq. (1) it means that the local kinetic function  $f$  depends on the lattice temperature  $T$ . We get  $\partial_T f < 0$  when temperature suppresses the vertical transport. Since the thermal diffusion length  $\ell_T$  is typically much larger than the device width  $w$ , the heat dynamics in the device can be modelled by the two-dimensional equation

$$c\rho w \frac{\partial T}{\partial t} = \kappa w \Delta_{\perp} T + Ju - \gamma(T - T_{\text{ext}}), \quad (3)$$

$$\Delta_{\perp} \equiv \partial_x^2 + \partial_y^2.$$

Here  $T$  corresponds to the mean value of temperature along the device vertical direction,  $c$ ,  $\rho$ , and  $\kappa$  are specific heat, density, and heat conductivity of the semiconductor material, respectively. The second and the third terms on the right-hand side of Eq. (3) describe Joule heating and cooling due to contact with environment, respectively.  $T_{\text{ext}}$  is the temperature of the external cooling reservoir. For multilayer structures with classical transport,  $T_{\text{ext}}$

is usually a room temperature. The coefficient  $\gamma$  is a heat transfer coefficient (per unit square of the structure) that characterizes the efficiency of external cooling. The characteristic relaxation time  $\tau_T$ , diffusion length  $\ell_T$ , and propagation velocity  $v_T$  are given by

$$\tau_T \equiv \frac{c\rho w}{\gamma}, \quad \ell_T \equiv \sqrt{\frac{\kappa w}{\gamma}}, \quad v_T \equiv \frac{\ell_T}{\tau_T} = \sqrt{\frac{\kappa \gamma}{c^2 \rho^2 w}}. \quad (4)$$

The modified model is given by the following set of equations:

$$\frac{\partial a}{\partial t} = \nabla_{\perp} (D_a(a) \nabla_{\perp} a) + f(a, u, T), \quad (5)$$

$$\tau_T \frac{\partial T}{\partial t} = \ell_T^2 \Delta_{\perp} T + (Ju/\gamma + T_{\text{ext}} - T), \quad (6)$$

$$\tau_u \frac{du}{dt} = U_0 - u - R \int_S J(a, u, T) dx dy. \quad (7)$$

The variable  $T$  plays a role of the second inhibitor.

In the following we assume that the device is elongated along the  $x$  direction ( $L_x \gg L_y$ ) and take only this lateral dimension into account. We also neglect direct effect of temperature on the current density  $J$  in Eq. (7).

### III. CURRENT FILAMENT AND MECHANISM OF ITS MOTION

Current density filament in a long structure represents a domain of the high current density state embedded into a low current density state (Fig. 2). The width of the filament wall  $\ell_f$  is of the order of  $\ell_f \sim \sqrt{D_a/\partial_a f}$ .<sup>7</sup> For  $T = T_{\text{ext}}$  the voltage  $u_{\text{co}}$  over the device with steady filament is chosen by the condition known as ‘‘equal area rule’’<sup>2,5</sup>

$$\int_{a_{\text{off}}}^{a_{\text{on}}} f(a, u_{\text{co}}, T = T_{\text{ext}}) D_a(a) da = 0, \quad (8)$$

which ensures that production and annihilation of the inhibitor  $a$  in the filament wall compensate each other. When the integral in (8) is positive or negative, the balance is broken, and the filament walls move in such a way that the high current density state or the low current density state, respectively, expand. Since  $\partial_u f > 0$ , the filament expands for  $u > u_{\text{co}}$  and shrinks for  $u < u_{\text{co}}$ . The filament has neutral stability with respect to the lateral shift when  $T$  is kept constant.<sup>8</sup>

The current-voltage characteristic of the filament in long structure is practically vertical<sup>2,5,8,41</sup> and bends in the upper and lower parts when the filament becomes narrow (Fig. 1). The bent parts correspond to current density intervals  $[J_{\text{off}}; J_{\text{off}} + (\ell_f/L_x)J_{\text{on}}]$  and  $[J_{\text{on}} - (\ell_f/L_x)J_{\text{on}}; J_{\text{on}}]$ , where  $J_{\text{on}}$  and  $J_{\text{off}}$  are current densities in the high current density state and the low current density state, respectively. These intervals are negligible for  $L_x \gg \ell_f$ .<sup>2,8,41</sup>

The current filament is stable for sufficiently large load resistance  $R$  and small relaxation time  $\tau_u$ .<sup>8,10</sup> We assume

that  $\tau_u \ll \tau_a, \tau_T$ , and hence Eq. (7) essentially represents a constraint imposed on the dynamics determined by Eqs. (5), (6). Without loss of generality we can also assume that the regime of the external circuit is close to the current-controlled regime:  $U_0 \gg u_{co}$  and the total current  $I \approx U_0/R$  is constant. The width of the filament is directly proportional to the total current  $I$

$$W = \frac{1}{L_y} \frac{I - L_x L_y \cdot J_{\text{off}}}{J_{\text{on}} - J_{\text{off}}} \approx \frac{1}{L_y} \frac{I}{J_{\text{on}}}, \quad (9)$$

where the last equality takes into account that typically  $J_{\text{on}} \gg J_{\text{off}}$ .

Qualitatively, the mechanism of the filament motions in presence of self-heating is the following. With increase of temperature the stationary balance (8) within the filament wall is broken due to the temperature dependence of the local kinetic function  $f(a, u, T)$ . As far as the temperature profile  $T(x)$  is symmetric, the left and right walls of the filament are equal and filament would either expand or shrink. This is forbidden since the total current is conserved by the global constraint (7). Increase of temperature is compensated by deviation of  $u$  from  $u_{co}$  in such a way that the stationary balance within the filament wall is restored. Since  $\partial_u f > 0$  and  $\partial_T f < 0$ , the voltage increases, but the filament stays steady. In contrast, for antisymmetric temperature fluctuation the balance is disturbed differently in the left and right filament walls, becoming positive at one side and negative at another side. Potentially, this spontaneous instability leads to the motion of a filament as a whole preserving the total current. In the traveling filament the temperature at the back edge exceeds the temperature at the leading edge due to the heat inertia of the semiconductor structure. Hence the filament motion becomes self-sustained.

Below we present an analytical theory of this effect. The theory is based on the following assumptions:

(i) the effect of self-heating is small and can be considered as a perturbation, hence the local kinetic function can be linearized near  $T = T_{\text{ext}}$  and  $u = u_{co}$  as

$$f(a, u, T) = f(a, u_{co}, T = T_{\text{ext}}) + (u - u_{co}) \partial_u f + (T - T_{\text{ext}}) \partial_T f; \quad (10)$$

(ii) the transverse dimension of the semiconductor structure is large in the sense that  $L_x \gg \ell_f, \ell_T$ , therefore only wide filaments with  $W \gg \ell_f$  are relevant and the effect of boundaries is negligible;

(iii) the width of the filament wall  $\ell_f$  is much smaller than the thermal diffusion length  $\ell_T$  and therefore the temperature variation within the filament walls can be neglected.

## IV. STATIONARY MOTION OF A FILAMENT: GENERAL PROPERTIES

### A. Model equations in the co-moving frame

For stationary motion of a filament with a constant velocity  $v$  the solution of Eqs. (5), (7), (6) has a form:

$$a(x, t) = a(x - vt), \quad T(x, t) = T(x - vt), \quad u = \text{const.} \quad (11)$$

In the co-moving frame  $\xi = x - vt$ , Eqs. (5), (7), (6) are

$$(D_a(a)a')' + v a' + f(a, u, T) = 0, \quad (12)$$

$$\ell_T^2 T'' + v \tau_T T' + (Ju/\gamma + T_{\text{ext}} - T) = 0, \quad (13)$$

$$U_0 - u - R L_y \langle J(a, u) \rangle = 0. \quad (14)$$

Here the prime (...) denotes the derivative with respect to  $\xi$  and angular brackets (...) denote integration over  $\xi$ . For the sufficiently large  $L_x$  the boundary conditions are given by

$$a(\xi) \rightarrow a_{\text{off}}(u), \quad T(\xi) \rightarrow T_\star \quad \text{for} \quad \xi \rightarrow \pm\infty, \quad (15)$$

where

$$T_\star \equiv T_{\text{ext}} + J_{\text{off}}(u_{co})u_{co}/\gamma \quad (16)$$

is the stationary temperature corresponding to the low current density state.

### B. Filament velocity and voltage over the structure

In order to calculate the velocity of the filament and the voltage on the structure with traveling filament, we note that for given  $u$  and  $T$  both filament walls can be treated as propagating fronts in bistable medium and use the standard formula<sup>25,31,41</sup>

$$v = \frac{2 \int_{a_{\text{off}}}^{a_{\text{on}}} f(a, u, T) D_a(a) da}{\langle D_a(a)(a'_0)^2 \rangle}, \quad (17)$$

where the filament profile is approximated by the stationary profile  $a_0(x)$ . Eq. (17) implies that the velocity  $v$  is proportional to the disbalance of production and annihilation of the activator  $a$  in the filament wall. Here  $T$  is the temperature within the filament wall under consideration, which is taken as constant according to the assumption  $\ell_f \ll \ell_T$ . The factor 2 in the nominator appears because  $a_0$  corresponds to the pattern that consists of two fronts. Positive and negative velocities correspond to the propagation of the high current density state into the low current density state and *vice versa*, respectively.

Linearizing the local kinetic function according to Eq. (10) and taking into account Eq. (8), we obtain

$$v(u, T) = \frac{2}{\langle D_a(a)(a'_0)^2 \rangle} \times \int_{a_{\text{off}}}^{a_{\text{on}}} [(u - u_{co}) \partial_u f + (T - T_{\text{ext}}) \partial_T f] D_a(a) da. \quad (18)$$

Hereafter, all derivatives are taken at  $u = u_{\text{co}}$  and  $T = T_{\text{ext}}$ .

Equation (18) should be applied separately to the left and the right filament walls. In terms of Eq. (18) the respective velocities have the same absolute value but different signs

$$v(u, T_R) = -v(u, T_L), \quad (19)$$

where  $T_R$  and  $T_L$  are temperatures at the right and the left walls, respectively. Equations (18) and (19) yield together

$$v = \frac{T_R - T_L}{\langle D_a(a) (a'_0)^2 \rangle} \int_{a_{\text{off}}}^{a_{\text{on}}} \partial_T f D_a(a) da, \quad (20)$$

$$u = u_{\text{co}} + B \left( \frac{T_L + T_R}{2} - T_{\text{ext}} \right), \quad (21)$$

$$B \equiv - \frac{\int_{a_{\text{off}}}^{a_{\text{on}}} \partial_T f D_a(a) da}{\int_{a_{\text{off}}}^{a_{\text{on}}} \partial_u f D_a(a) da}.$$

According to Eqs. (20), (21) the filament velocity is proportional to the difference of temperatures at the filament edges ( $T_L - T_R$ ), while the voltage deviation from  $u_{\text{co}}$  is proportional to the mean value  $(T_L + T_R)/2$ . For  $\partial_T f < 0$  the coefficient  $B$  is positive, and hence the voltage increases with the increase of temperature. The filament moves to the right ( $v > 0$ ) when  $T_L > T_R$  and to the left ( $v < 0$ ) when  $T_L < T_R$ .

It is worth to mention that formula (20) derived for the wide filament with narrow walls is a special case of the general expression

$$v = - \frac{\langle \partial_T f D_a(a) T(\xi) a'_0 \rangle}{\langle D_a(a) (a'_0)^2 \rangle}, \quad (22)$$

which is applicable for any filament shape and temperature profile  $T(\xi)$  satisfying the boundary condition (15). Similar to Eq. (17), equation (22) can be obtained by multiplying Eq. (12) by  $D_a(a)a'$ , integrating over  $\xi$  and using the expansion (10).

Eqs. (20), (21) do not refer exclusively to the case of Joule self-heating. They are applicable regardless of the origin of the inhomogeneous temperature profile in the semiconductor structure. We conclude that when temperature suppresses the vertical transport ( $\partial_T f < 0$ ), as it happens in case of impact ionization mechanism of S-type characteristic, the filament generally moves against the temperature gradient. In the case when the influence of heating is positive ( $\partial_T f > 0$ ), as it happens, for example, when the thermogeneration mechanism is involved, the filament moves along the temperature gradient.

### C. Temperature profile in the moving filament

For a filament with narrow walls ( $\ell_f \ll \ell_T$ ) the heat equation (13) is piecewise linear and the temperature profile  $T(\xi)$  can be found analytically (see Appendix).

Consequently, the temperatures  $T_L$  and  $T_R$  can be presented explicitly as functions of the filament velocity  $v$  and width  $W$ . It is convenient to introduce the normalized difference and the sum of  $T_L$  and  $T_R$ :

$$\Delta_{LR} \equiv \frac{T_L - T_R}{T^* - T_*}, \quad \Sigma_{LR} \equiv \frac{T_L + T_R - 2T_*}{T^* - T_*}, \quad (23)$$

where the temperatures  $T^*$  and  $T_*$  are stationary uniform solutions of the heat equation (6) corresponding to uniform on and off states, respectively:<sup>43</sup>

$$T^* = T_{\text{ext}} + J_{\text{on}}(u_{\text{co}}) u_{\text{co}}/\gamma, \quad (24)$$

and  $T_*$  is defined by Eq. (16). Typically  $T_* \approx T_{\text{ext}}$ .

From the solution (A.2) of the heat equation we obtain

$$\Delta_{LR} = \frac{1}{\sqrt{1 + \tilde{v}^2}} \left( \tilde{v} - \exp\left(-\tilde{W}\sqrt{1 + \tilde{v}^2}\right) \times \left[ \tilde{v} \cosh\left(\tilde{W}\tilde{v}\right) + \sqrt{1 + \tilde{v}^2} \sinh\left(\tilde{W}\tilde{v}\right) \right] \right), \quad (25)$$

$$\Sigma_{LR} = 1 - \frac{1}{\sqrt{1 + \tilde{v}^2}} \exp\left(-\tilde{W}\sqrt{1 + \tilde{v}^2}\right) \times \left[ \tilde{v} \sinh\left(\tilde{W}\tilde{v}\right) + \sqrt{1 + \tilde{v}^2} \cosh\left(\tilde{W}\tilde{v}\right) \right], \quad (26)$$

where

$$\tilde{v} = \frac{v}{2v_T}, \quad \tilde{W} = \frac{W}{\ell_T}.$$

The dependencies  $\Delta_{LR}(v, W)$  and  $\Sigma_{LR}(v, W)$  are shown in Fig. 3. The temperature difference is equal to zero for  $v = 0$ , when the temperature profile is symmetric, and reaches maximum at a certain value of  $v$  [Fig. 3(a)]. The temperature difference decreases with further increase of  $v$  and vanishes for large velocities ( $v \gg W/\tau_T$ ) when the filament moves too fast to heat the semiconductor structure. The average temperature and, according to Eq. (21), the voltage  $u$  monotonically decrease as  $v$  increases [Fig. 3(b)]. Hence the onset of filament motion is always accompanied by a certain voltage drop. Both  $(T_L - T_R)$  and  $(T_L + T_R)$  increase with filament width  $W$  for a given  $v$ .

## V. SELF-CONSISTENT DETERMINATION OF FILAMENT VELOCITY

In the regime of Joule self-heating, the stationary filament motion with a certain velocity occurs when the moving filament generates the temperature profile with the temperature difference  $(T_L - T_R)$  which is exactly needed to support this motion. Combining Eqs. (20), (23), and (25), we obtain a transcendental equation for the filament velocity  $v$ :

$$\frac{v}{v_0} = \Delta_{LR}(v, W), \quad (27)$$

$$v_0 \equiv - \frac{T^* - T_*}{\langle D_a(a) (a'_0)^2 \rangle} \int_{a_{\text{off}}}^{a_{\text{on}}} \partial_T f D_a(a) da. \quad (28)$$

Here  $v_0$  is the upper limit of the filament velocity which is achieved for  $T_L - T_R = T^* - T_*$ . This velocity characterizes the effect of temperature on the filament dynamics. The function  $\Delta_{LR}$  is explicitly given by Eq. (25).  $\Delta_{LR}$  is odd with respect to  $v$ , reflecting the symmetry between left and right directions of the filament motion. Hence nontrivial solutions  $v^* \neq 0$  of Eq. (27) always come in pairs  $(v^*, -v^*)$ . Having this in mind, below we discuss only nonnegative solutions  $v \geq 0$ . Note that  $v_0 < 0$  for  $\partial_T f > 0$  (positive influence of temperature on vertical transport), and therefore Eq. (28) has only trivial solution  $v = 0$ : filament motion is not possible. We shall focus on the case  $\partial_T f < 0$  when  $v_0 > 0$ .

It is immediately evident from Fig. 3(a) that Eq. (27) has either one or two nonnegative roots depending on  $v_0$  and  $W$ . Solution  $v^* = 0$ , corresponding to a steady filament, exists for all parameter values. Nontrivial solution  $v^* > 0$ , that corresponds to the traveling filament, exists if

$$v_0 \left. \frac{d\Delta_{LR}}{dv} \right|_{v=0} > 1. \quad (29)$$

When the root  $v = 0$  is unique, the corresponding stationary filament is stable because  $\Delta_{LR}(v) < v/v_0$  for  $v > 0$ . This inequality means that traveling filament generates a temperature difference  $(T_L - T_R)$  which is not sufficient to support its motion. The situation changes when the condition (29) is met: in this case  $\Delta_{LR}(v) > v/v_0$  for  $v > 0$ , and the steady solution is unstable. It means that the steady filament loses stability simultaneously with appearance of the nontrivial solution  $v^* > 0$  which corresponds to traveling filament. Hence, Eq. (29) represents a condition for spontaneous onset of the filament motion. We discuss the bifurcation from static to traveling filament in more details in the next section.

Traveling filament is stable because  $\Delta_{LR}(v) > v/v_0$  for  $v < v^*$  and  $\Delta_{LR}(v) < v/v_0$  for  $v > v^*$ . Indeed, these inequalities mean that if  $v$  decreases the temperature difference  $(T_L - T_R)$  increases and hence according to (20) the filament velocity should increase again. In the same way, with increase of  $v$  the difference  $(T_L - T_R)$  decreases and therefore the filament slows down.

In Fig. 4(a) we present numerical solutions  $v(W)$  of Eq. (27) for different values of the parameter  $v_0$ . For a given  $v_0$  the motion is possible for filaments whose width exceeds a certain threshold  $W_{th}(v_0)$  (Fig. 5). With increase of  $W$  the filament velocity increases and eventually saturates. We discuss the analytical approximations of the front velocity in Sec. VII and Sec. VIII.

In Fig. 4(b) we present the voltage  $u$  in the regime of current filamentation obtained by substituting numerical solutions of Eq. (27) into Eqs. (21), (26). The normalized deviation of  $u$  from  $u_{co}$

$$\Delta \tilde{u} = 2 \frac{B^{-1}(u - u_{co}) - (T_* - T_{ext})}{T^* - T_*} \quad (30)$$

is shown, where  $B$  is determined by Eq. (21). The voltage drop, clearly visible on curves 2–7, is associated with the

onset of filament motion. With further increase of  $W$  the voltage increases again. Curve 1 is calculated for  $v_0/v_T = 2.1$ , which is close to the threshold value  $v_0/v_T = 2$ , and practically coincides with the curve for a static filament. Since the filament width  $W$  is directly proportional to the total current  $I$  [see Eq. (9)], Fig. 4(b) actually represents the current-voltage characteristic of the structure with traveling filament.

## VI. ONSET OF THE FILAMENT MOTION

To analyze the onset of filament motion and propagation of slow filaments we expand  $\Delta_{LR}$  with respect to  $v/v_T$  up to the second order:

$$\Delta_{LR}(v, W) \approx \frac{v}{2v_T} \left( 1 - \frac{1}{8} \left( \frac{v}{v_T} \right)^2 \right) A(W), \quad (31)$$

$$A(W) \equiv \left[ 1 - \left( 1 + \frac{W}{\ell_T} \right) \exp \left( -\frac{W}{\ell_T} \right) \right].$$

In this case the temperature profile is close to the symmetric stationary profile given by Eq. (A.4).

Substituting Eq. (31) in Eq. (29), we obtain an explicit condition for the onset of filament motion

$$\frac{v_0}{2v_T} A(W) > 1. \quad (32)$$

This condition can be further simplified for narrow and wide filaments:

$$\frac{v_0}{4v_T} \left( \frac{W}{\ell_T} \right)^2 > 1 \quad \text{for } W \ll \ell_T, \quad (33)$$

$$\frac{v_0}{2ev_T} \left( \frac{W}{\ell_T} + e - 3 \right) > 1 \quad \text{for } W \sim \ell_T, \quad (34)$$

$$\frac{v_0}{2v_T} > 1 \quad \text{for } W \gg \ell_T, \quad (35)$$

where  $e$  is the natural logarithmic base. Since  $A(W) < 1$ , it follows from Eq. (32) that regardless to the filament width  $W$  the filament motion is not possible if  $v_0 < 2v_T$ . If  $v_0 > 2v_T$ , the filaments whose width  $W$  overcomes the threshold  $W_{th}$  determined by Eq. (32) start to move, whereas smaller filaments remain steady. The dependence of  $W_{th}$  on  $v_0/v_T$  is shown in Fig. 5, curve 1. This dependence can be approximated as

$$W_{th} \approx 2\ell_T \sqrt{\frac{v_T}{v_0}} \quad \text{for } W_{th} \ll \ell_T, \quad (36)$$

$$W_{th} \approx \ell_T \left( 2e \frac{v_T}{v_0} + 3 - e \right) \quad \text{for } W_{th} \sim \ell_T, \quad (37)$$

$$W_{th} \approx -\ell_T \ln \left( 1 - \frac{2v_T}{v_0} \right) \quad \text{for } W_{th} \gg \ell_T. \quad (38)$$

The bifurcation to traveling filament resembles a supercritical pitchfork bifurcation:<sup>44</sup> at the bifurcation point  $W = W_{th}$  the static solution becomes unstable and

simultaneously two stable branches corresponding to the filaments traveling to the left and to the right appear [Fig. 4(a)]. This bifurcation can be understood in terms of stability analysis of the current filament performed in Ref. 8 for standard two-component model (1), (2): The spectrum of eigenmodes of a static filament includes a neutral mode  $\Psi_T$  with zero eigenvalue  $\lambda_T = 0$  which corresponds to translation. Existence of this neutral mode reflects the translation invariance of a static filament on a large spatial domain. In the extended model (5), (6), (7) the bifurcation to traveling filament is characterized by symmetry breaking when  $\lambda_T$  becomes positive. This becomes possible due to the coupling between the master equation (5) and the heat equation (6) when  $\partial_T f < 0$ . Note that for  $\partial_T f > 0$  the eigenvalue of the translation mode  $\lambda_T$  becomes negative. This corresponds to self-pinning of the filament.

## VII. PROPAGATION OF SLOW FILAMENTS

Substituting Eq. (31) into Eq. (27) we obtain an explicit equation for the filament velocity which is applicable for slow fronts:

$$v(W) = 2v_T \sqrt{\frac{v_0}{v_T} A(W) - 2}, \quad (39)$$

where  $A(W)$  is defined in Eq. (31). The asymptotic value is given by

$$v \rightarrow 2v_T \sqrt{\frac{v_0}{v_T} - 2} \quad \text{for} \quad \frac{W}{\ell_T} \rightarrow \infty. \quad (40)$$

Eq. (39) approximates  $v(W)$  with an accuracy of 10% up to the parameter value  $v_0/v_T = 3$  [curve 2 on Fig. 4(a)], despite it is derived for  $v \ll v_T$ . This wide range of applicability is due to particular smooth behavior of  $\Delta_{LR}(v)$  to the left of its peak value [see Fig. 3(a)].

## VIII. PROPAGATION OF FAST FILAMENTS

In the limit  $v \gg v_T$  the temperature profile is strongly asymmetric [see Eq. (A.5)], and the temperature at the leading edge is close to  $T_*$ . The expression (25) can be expanded with respect to  $v_T/v$ :

$$\Delta_{LR}(v, W) = 1 - \exp\left(-\frac{W}{v\tau_T}\right) - \left(\frac{v_T}{v}\right)^2 \left[2 - \exp\left(-\frac{W}{v\tau_T}\right)\right]. \quad (41)$$

According to Eq. (A.3) the characteristic scale of the temperature profile for the fast filament is determined by  $(\lambda^+)^{-1} \approx v\tau_T$  which exceeds  $\ell_T$ . To keep the diffusion correction, we expand up to the second order.

Analytical results are available for the case of a narrow filament ( $W \ll v\tau_T$ ) and a wide filament ( $W \gg v\tau_T$ ).

In the first case ( $W \ll v\tau_T$ ) the temperature inside the filament increases linearly, and  $T_L$  is much smaller than  $T^*$ . For  $W/v\tau_T \ll 1$ , equation (41) reduces to

$$\Delta_{LR}(v, W) \approx \frac{W}{\ell_T} \left(\frac{v_T}{v}\right) - \left(\frac{v_T}{v}\right)^2. \quad (42)$$

Substituting (42) into Eq. (27) we obtain the filament velocity

$$v(W) \approx \sqrt{\frac{Wv_0}{\tau_T}} - \frac{\ell_T v_T}{2W} \quad \text{for} \quad W \ll v\tau_T. \quad (43)$$

Note that in Eq. (43) the leading term does not depend on the heat diffusion.

In the case of wide filament ( $W \gg v\tau_T$ ) the temperature at the back edge is close the maximum value  $T^*$ . The front velocity is approximated by

$$v(W) \approx v_0 - \frac{2v_T^2}{v_0} - \exp\left(-\frac{W}{v_0\tau_T}\right) \left[v_0 - \frac{2v_T^2}{v_0}\right] \quad \text{for} \quad W \gg v\tau_T \quad (44)$$

and saturates at

$$v \rightarrow v_0 - \frac{2v_T^2}{v_0} \quad \text{for} \quad \frac{W}{v_0\tau_T} \rightarrow \infty.$$

## IX. DISCUSSION

### A. Scales hierarchy - which limiting case is relevant?

The thermal relaxation time  $\tau_T$  of the semiconductor structure can be straightforwardly determined in experiment. Therefore it is convenient to use it as basic parameter and to express  $\ell_T$  and  $v_T$  via  $\tau_T$ . Depending on the structure width and design, the effective value of  $\tau_T$  varies from 100-200 ns for transistorlike structures of electrostatic discharge protections devices<sup>39</sup> (the structure width  $w \sim 10 \mu\text{m}$ ) to  $\sim 10$ -100 ms for power devices (the structure width  $w \sim 100$ -500  $\mu\text{m}$ )<sup>40</sup>. It follows from Eq. (4) that parameters  $\ell_T$  and  $v_T$  are connected to  $\tau_T$  via

$$\ell_T = \sqrt{D_T \tau_T}, \quad v_T = \sqrt{\frac{D_T}{\tau_T}}, \quad D_T \equiv \frac{\kappa}{c\rho}, \quad (45)$$

where the thermal diffusivity  $D_T$  depends only on material parameters. We take  $D_T = 0.92 \text{ cm}^2/\text{s}$  and  $D_T = 0.25 \text{ cm}^2/\text{s}$  for Si and GaAs, respectively. Consequently,  $\ell_T$  and  $v_T$  are of the order of 100  $\mu\text{m}$  and  $10^3 \text{ cm/s}$ , respectively, for small devices ( $\tau_T \sim 100 \text{ ns}$ ,  $w \sim 10 \mu\text{m}$ ). We obtain 1 mm and 10 cm/s, respectively, for large power devices ( $\tau_T \sim 10 \text{ ms}$ ,  $w \sim 100 \mu\text{m}$ ). Hence in most devices the filament width  $W$  is of the order of the thermal diffusion length  $\ell_T$  or smaller, and  $\ell_T$  is smaller but comparable to the transverse dimension of the structure  $L$ . In particular, it implies that in the regime of

self-heating the maximum temperature in the current filament is much smaller than  $T^*$ . For  $W \lesssim \ell_f$  and sufficiently far from the bifurcation point  $v_0 = 2v_T$  the filament velocity is well described by the formula (43), where the second term can be neglected.

### B. Stimulating the filament motion

Motion of the filament delocalizes heating of semiconductor structure and thus is desirable in applications. Generally, the start of the filament motion becomes easier with increase of  $v_0$  and decrease of  $v_T$  and  $\ell_T$  (see Eq. (32) and Fig. 5, curve 1). However, these parameters cannot be varied independently. Below we focus on the effect of the structure parameters which enter our model: the heat transfer coefficient  $\gamma$  and the structure width  $w$ .

Curve 2 in Fig. 5 shows the threshold filament width  $W_{\text{th}}$  normalized by the quantity  $(D_T^2 \tau_T / v_0)^{1/3}$  which does not depend on the heat transfer coefficient  $\gamma$ . Taking into account that  $v_T / v_0 \sim \gamma^{3/2}$ , we conclude that decrease of  $\gamma$  makes the onset of the filament motion easier. This occurs due to the increase of  $v_0$  which, according to Eqs. (16), (24), (28), scales as  $v_0 \sim \gamma^{-1}$ . However, easy start of the filament motion in structures with inefficient cooling comes at the price of increasing the temperature in the filament, which makes static filaments more dangerous.

Curve 3 in Fig. 5 shows  $W_{\text{th}}$  normalized by the quantity  $(D_T / v_0)^{1/2}$  which does not depend on  $w$ . Since  $v_T / v_0 \sim w^{-1/2}$ , we see that the dependence of  $W_{\text{th}}$  on  $w$  is nonmonotonic. Physically relevant situation  $W \lesssim \ell_T$  corresponds to the left part of the curve 3 where  $W_{\text{th}}$  increases with  $w$ . The effect is due to increase of  $\ell_T \sim w^{1/2}$ . Thus, for the fixed value of  $v_0$ , thinner structures are preferable for the filament motion.

### C. Transient behavior

Static current filament typically appears due to the spatial instability of the uniform state on the middle branch of current-voltage characteristic (see Fig. 1). This occurs<sup>7</sup> on the time scale  $\tau_a$  which is typically smaller than the thermal time scale  $\tau_T$ . First the voltage settles at  $u = u_{\text{co}}$ , and only then the temperature starts to increase. According to Eq. (21) the Joule heating is accompanied by increase of  $u$ . As soon as the static filament gets hot, the bifurcation to the traveling filament occurs, provided that the condition (29) is satisfied. The onset of filament motion leads to a certain voltage drop, though  $u$  remains larger than  $u_{\text{co}}$  [see Eq. (21) and Fig. 4(b)]. The motion can start before the stationary temperature profile in the static filament is established, but the non-monotonic dynamics of  $u$  remains qualitatively the same.

### D. Self-motion and self-pinning

As it has been pointed out in Sec. VI, we predict, instead of self-motion, self-pinning of the filament at its initial location due to the Joule self-heating in the case  $\partial_T f > 0$ . For example, it happens when the temperature becomes high enough for thermogeneration to set in. This typically precedes thermal destruction of the semiconductor structure due to local overheating. Eq. (20) also suggests an experimental method to distinguish between positive ( $\partial_T f > 0$ ) and negative ( $\partial_T f < 0$ ) influence of temperature on vertical transport by observing the filament dynamics in externally applied temperature gradient: filaments move along and against the temperature gradient for  $\partial_T f > 0$  and  $\partial_T f < 0$ , respectively.

### E. Motion of low-current filaments

S-shaped current-voltage characteristic exhibits formal duality between high current density and low current density branches. Therefore apart from high-current filaments, there are patterns in form of low-current filaments: domains of low current density embedded into on state.<sup>5,8</sup> Such filaments correspond to the upper part of the filamentary current-voltage characteristic (Fig. 1), where average current density is close to  $J_{\text{on}}$ . In the case  $\partial_T f < 0$  low-current filaments also undergo the bifurcation from static to traveling filament. Expressions (20), (21) remain valid as they are, whereas in Eqs. (25), (26)  $T^*$  and  $T_*$  should be exchanged. The onset of motion results in the increase, rather than decrease, of the voltage in this case. Duality between on and off states is broken when vertical transport is suppressed near the structure boundary due to a certain process at the lateral edge of the semiconductor structure, e.g., surface recombination or surface leak in the  $p$ - $n$  junction. (This effect can be modelled by Dirichlet boundary conditions  $a = 0$  imposed on the variable  $a$  at  $x = 0, L_x$ .<sup>5</sup>) In this case the effect of boundaries can not be neglected for average current densities close to  $J_{\text{on}}$  even in the limit  $L_x \gg \ell_f$ . The current-voltage characteristic, instead of hysteresis, exhibits a continuous crossover from the filamentary branch to the branch of quasiuniform high current density states at high current.<sup>5</sup> Then only high-current filaments are observable.

### F. Reaction-diffusion models for traveling spots

The model (5), (6), (7) belongs to the same class of three-component reaction-diffusion models as models for traveling spots in active media discussed in Refs. 45,46, 47,48,49,50. In contrast to the common two-component activator-inhibitor model,<sup>22,31</sup> three-component models are capable to describe localized traveling patterns not only on a one-dimensional spatial domain, but also on spatial domains of higher dimensions.<sup>45,46</sup> The transition

from static to traveling spot takes place with increase of the relaxation time of the first inhibitor,<sup>45</sup> in the same way as it occurs in the common two-component model of pulse propagation in excitable media.<sup>31</sup> The second fast long-range inhibitor plays an essential role only in the two-dimensional or three-dimensional case: it prevents lateral spreading of the traveling spot which otherwise destroys the spatially localized solution and eventually leads to development of a spiral wave.<sup>45,46</sup>

This additional inhibition can be either global<sup>45</sup> or local.<sup>46</sup> In the first case the inhibitor has the same value in the whole system. This value depends on the mean value of other dynamical variables in the system and is governed by an integro-differential equation. This corresponds to the global coupling of a spatially extended nonlinear system. In the second case the additional inhibitor is governed by a conventional reaction-diffusion equation. For traveling spots, the difference between these two cases becomes crucial only when several spots are considered on a two or higher dimensional domain: the system of several spot is unstable when the additional inhibition is global, but becomes stable when it is local.<sup>46</sup> This difference vanishes when only one spot is present, or the spatial domain is one-dimensional.<sup>46</sup> Global coupling through the gas phase occurs in the surface reactions<sup>51,52,53,54</sup> and can be implemented as global feedback loop in the light-sensitive Belousov-Zabotinsky reaction<sup>55,56</sup>. Implementation of the respective control loop has allowed to observe localized traveling patterns in these systems.<sup>54,56</sup>

In contrast to the three-component models discussed in Refs. 45,46, in the model (5), (6), (7) both inhibitors are needed for the onset of filament motion already in the one-dimensional case. Consequently, the bifurcation to traveling filament is also different. This reflects the fact that we start with a stationary pattern in a bistable medium with fast global inhibition (voltage  $u$ ). This global inhibition is due to the external circuit and represents an inherent feature of spatio-temporal dynamics of a bistable semiconductor: For any evolution of the current density pattern which is accompanied by the variation of the total current, the voltage at an external series resistance changes, causing the variation of the voltage across the device. This inhibition is crucial for the existence of current filaments which become unstable when the global coupling is eliminated by operating the device in the voltage-controlled regime.<sup>2,8,10</sup> The motion of the filament is induced by the effect of another slow diffusive inhibitor (temperature  $T$ ). Similar nonlinear mechanism causes the motion of current filaments obtained by numerical simulations in Refs. 23,47. However, Refs. 23,47 focus on a specific type of multilayer thyristorlike structures. The model of these devices<sup>27</sup> assumes that the second inhibitor is a certain internal voltage, not a temperature.

It is worth to mention, that self-heating may also trigger temporal relaxation-type oscillations of a current-density filament. This effect has been observed in a re-

versely biased  $p-i-n$  diode and is explained by a similar three-component reaction-diffusion model.<sup>57</sup>

## X. SUMMARY

Joule self-heating of a current density filament in a bistable semiconductor structure might result in the onset of lateral motion. This occurs when increase of temperature has negative impact on the vertical (cathode-anode) transport. Such negative feedback takes place when bistability of semiconductor structure is related to the avalanche impact ionization, because the impact ionization rate decreases with temperature.<sup>4</sup> Examples of such devices are avalanche transistors,<sup>18</sup> reversely biased  $p-i-n$  diodes in the regime of avalanche injection, electrostatic discharge protection devices operated in the avalanche regime,<sup>28</sup> multilayer thyristorlike structures.<sup>21,27</sup> Traveling filaments can be consistently described by a generic nonlinear model (5), (6), (7).

Generally, filaments move against the temperature gradient with a velocity proportional to the temperature difference at the filament edges [Eq. (20)]. In the regime of Joule self-heating the strength of coupling between the master equation (5), which controls the current density dynamics, and the heat equation (6) can be characterized by single parameter  $v_0$  [Eq. (28)], which has a dimension of velocity. The filament velocity  $v$  is determined by the transcendental equation (27). The condition for the spontaneous onset of filament motion (29) depends on the ratio of  $v_0$  and the thermal velocity  $v_T$ , and on the ratio of the filament width  $W$  and the thermal diffusion length  $\ell_f$ . Filament motion is never possible for  $v_0 < 2v_T$ . For  $v_0 > 2v_T$ , static filaments whose width  $W$  exceeds a certain threshold  $W_{th}$  [Eq. (32), curve 1 in Fig. 5] become unstable and start to travel. The filament velocity  $v$  and the voltage on the structure  $u$  are shown in Fig. 4. For most semiconductor structures  $W \lesssim \ell_T$ , and sufficiently far from the bifurcation point  $v_0 = 2v_T$  the filament velocity can be approximated by a truncated version of Eq. (43)

$$v \approx \sqrt{\frac{Wv_0}{\tau_T}}.$$

Heating of the static filament is accompanied by an increase of the voltage  $u$  [Eq. (21)]. With onset of the filament motion the voltage drops, but remains higher than the voltage  $u_{co}$  [Fig. 4(b)].

Our analytical theory does not cover narrow filaments, when the flat top of current density profile does not exist or the filament width  $W$  is comparable to the width of the filament wall  $\ell_f$ , as well as cylindrical filaments which appear when lateral dimensions of semiconductor structure  $L_x$  and  $L_y$  are comparable. However, the bifurcation from static to traveling filament and the mechanism of filament motion remain qualitatively the same in these cases.



### Acknowledgments

Stimulating discussions with S. Bychkhin, M. Denison and D. Pogany and the discussion of the results are gratefully acknowledged. The author thanks A. Mikhailov and V. Zykov for helpful discussions of the results. The work was supported by the Alexander von Humboldt Foundation.

### APPENDIX: SOLUTIONS OF THE HEAT EQUATION

Assuming that the front walls are thin, we present Eq. (13) as (see Fig. 2):

$$\begin{aligned} \ell_T^2 T'' + v \tau_T T' + (T^* - T) &= 0 & \text{(A.1)} \\ \text{for } -\frac{W}{2} < \xi < \frac{W}{2}, \\ \ell_T^2 T'' + v \tau_T T' + (T_* - T) &= 0 \\ \text{for } \xi < -\frac{W}{2} \text{ and } \xi > \frac{W}{2}. \end{aligned}$$

Here the middle of the filament is at  $\xi = 0$ .  $T_*$  and  $T^*$  are defined by Eqs. (16), (24). The solution of this piecewise linear equation is given by

$$\begin{aligned} T(\xi) &= T_* - (T^* - T_*) & \text{(A.2)} \\ &\times \frac{2\lambda^+}{\lambda^+ - \lambda^-} \sinh\left(\frac{\lambda^- W}{2}\right) \exp(\lambda^- \xi) \\ \text{for } \xi &> \frac{W}{2}, \\ T(\xi) &= T^* - \frac{T^* - T_*}{\lambda^+ - \lambda^-} \left( \lambda^+ \exp\left[\lambda^- \left(\xi + \frac{W}{2}\right)\right] \right. \\ &\quad \left. - \lambda^- \exp\left[\lambda^+ \left(\xi - \frac{W}{2}\right)\right] \right) \\ \text{for } \frac{W}{2} &< \xi < \frac{W}{2}, \\ T(\xi) &= T_* - (T^* - T_*) \\ &\times \frac{2\lambda^-}{\lambda^+ - \lambda^-} \sinh\left(\frac{\lambda^+ W}{2}\right) \exp(\lambda^+ \xi) \\ \text{for } \xi &< -\frac{W}{2}, \end{aligned}$$

where  $\lambda^+$  and  $\lambda^-$  are eigenvalues of Eq. (A.1):

$$\lambda^+ = \frac{1}{\ell_T} \left[ \sqrt{1 + \left(\frac{v}{2v_T}\right)^2} - \frac{v}{2v_T} \right], \quad \text{(A.3)}$$

$$\lambda^- = -\frac{1}{\ell_T} \left[ \sqrt{1 + \left(\frac{v}{2v_T}\right)^2} + \frac{v}{2v_T} \right].$$

Eqs. (A.2) allow to determine the temperature difference ( $T_L + T_R$ ) and the mean temperature  $(T_L + T_R)/2$  [Eqs. (23), (25), (26)] which are needed for self-consistent calculation of the front velocity  $v$  and the voltage  $u$ .

*Steady temperature profile.*— For  $v = 0$  we get  $\lambda^+ = -\lambda^- = 1/\ell_T$  and the corresponding symmetric temperature profile is given by

$$\begin{aligned} T(\xi) &= T_* + (T^* - T_*) \sinh\left(\frac{W}{2\ell_T}\right) \exp\left(-\frac{\xi}{\ell_T}\right) \\ \text{for } \xi &> \frac{W}{2}, & \text{(A.4)} \\ T(\xi) &= T^* - (T^* - T_*) \exp\left(-\frac{W}{2\ell_T}\right) \cosh\left(\frac{\xi}{\ell_T}\right) \\ \text{for } \frac{W}{2} &< \xi < \frac{W}{2}, \\ T(\xi) &= T_* + (T^* - T_*) \sinh\left(\frac{W}{2\ell_T}\right) \exp\left(\frac{\xi}{\ell_T}\right) \\ \text{for } \xi &< -\frac{W}{2}. \end{aligned}$$

*Temperature profile in the fast filament.*— For  $v \gg v_T$  we get  $\lambda^+ = (v\tau_T)^{-1}$ ,  $\lambda^- = -\infty$ . The corresponding profile is strongly asymmetric:

$$\begin{aligned} T(\xi) &= T_* \quad \text{for } \xi > \frac{W}{2}, & \text{(A.5)} \\ T(\xi) &= T^* - (T^* - T_*) \exp\left(\frac{2\xi - W}{2v\tau_T}\right) \\ \text{for } -\frac{W}{2} &< \xi < \frac{W}{2}, \\ T(\xi) &= T_* + 2(T^* - T_*) \sinh\left(\frac{W}{2v\tau_T}\right) \exp\left(\frac{\xi}{v\tau_T}\right) \\ \text{for } \xi &< -\frac{W}{2}. \end{aligned}$$

\* Electronic mail: rodin@physik.tu-berlin.de

<sup>1</sup> B. K. Ridley, Proc. Phys. Soc. London **82**, 954 (1963).

<sup>2</sup> A. F. Volkov and Sh. M. Kogan, Sov. Phys. Usp. **11**, 881 (1969) [Usp. Phys. Nauk **96**, 633 (1968)].

<sup>3</sup> V. L. Bonch-Bruevich, I. P. Zvyagin, and A. G. Mironov,

*Domain Electrical Instabilities in Semiconductors* (Consultant Bureau, New York, 1975).

<sup>4</sup> S. M. Sze, *Physics of Semiconductor Devices* (Wiley, New York, 1981).

<sup>5</sup> E. Schöll, *Nonequilibrium Phase Transitions in Semicon-*

- ductors (Springer-Verlag, Berlin Heidelberg, 1987).
- <sup>6</sup> M. Shaw, V. Mitin, E. Schöll, and H. Grubin, *The Physics of Instabilities in Solid State Electron Devices* (Plenum Press, New York, 1992).
  - <sup>7</sup> A. Wacker and E. Schöll, *J. Appl. Phys.* **78**, 7352 (1995).
  - <sup>8</sup> A. Alekseev, S. Bose, P. Rodin, and E. Schöll, *Phys. Rev. E* **57**, 2640 (1998).
  - <sup>9</sup> A. F. Volkov and Sh. M. Kogan, *Sov. Phys. JETP* **25**, 1095 (1967) [*Zh. Eksp. Teor. Fiz.* **52**, 1647 (1967)].
  - <sup>10</sup> F.G. Bass, V. S. Bochkov, Yu. Gurevich, *Sov. Phys. JETP* **31**, 972 (1970) [*Zh. Eksp. Teor. Phys.* **58**, 1814 (1970)].
  - <sup>11</sup> V. Novák, C. Wimmer, and W. Prettl, *Phys. Rev. B* **52**, 9023 (1995).
  - <sup>12</sup> F.-J. Niedernostheide, J. Hirschinger, W. Prettl, V. Novák, and H. Kostial, *Phys. Rev. B* **58**, 4454 (1998).
  - <sup>13</sup> V. Novák, J. Hirschinger, F.-J. Niedernostheide, W. Prettl, M. Cukr, and J. Oswald, *Phys. Rev. B* **58**, 13099 (1998).
  - <sup>14</sup> J. Hirschinger, F.-J. Niedernostheide, W. Prettl, and V. Novák, *Phys. Rev. B* **61**, 1952 (2000).
  - <sup>15</sup> G. Schwarz, C. Lehmann, and E. Schöll, *Phys. Rev. B* **61**, 10194 (2000).
  - <sup>16</sup> I. V. Varlamov, V. V. Osipov, and E. A. Poltoratsky, *Sov. Phys. Semicond.* **3**, 978 (1970) [*Fiz. Tekh. Poluprovodn.* **3**, 1162 (1969)].
  - <sup>17</sup> V. V. Osipov and V.A. Kholodnov, *Sov. Phys. Semicond.* **4**, 1033 (1971) [*Fiz. Techn. Poluprovodn.* **4**, 1216 (1970)].
  - <sup>18</sup> V. V. Osipov and V.A. Kholodnov, *Mikroelektronika* **2**, 529 (1973) (In Russian).
  - <sup>19</sup> D. Jäger, H. Baumann, and R. Symanczyk, *Phys. Lett. A* **117**, 141 (1986).
  - <sup>20</sup> A. V. Gorbatyuk, P. B. Rodin, *Solid-State Electron.* **35**, 1359 (1992).
  - <sup>21</sup> A. V. Gorbatyuk and F.-J. Niedernostheide, *Phys. Rev. B* **59**, 13157 (1999); **65**, 245318 (2002).
  - <sup>22</sup> B. S. Kerner, V. V. Osipov, *Autosolitons* (Kluwer Academic Publishers, Dordrecht, 1994).
  - <sup>23</sup> *Nonlinear Dynamics and Pattern Formation in Semiconductors and Devices*, edited by F.-J. Niedernostheide (Springer-Verlag, Berlin, 1995).
  - <sup>24</sup> K. Aoki, *Nonlinear Dynamics and Chaos of Semiconductors* (Institute of Physics Publishing, Bristol, 2000).
  - <sup>25</sup> E. Schöll, *Nonlinear Spatio-Temporal Dynamics and Chaos in Semiconductors* (Cambridge University Press, Cambridge, 2001).
  - <sup>26</sup> A. Wierschem, F.-J. Niedernostheide, A. Gorbatyuk, and H.-G. Purwins, *Scanning* **17**, 106 (1995).
  - <sup>27</sup> F.-J. Niedernostheide, B. S. Kerner, and H.-G. Purwins, *Phys. Rev. B* **46**, 7559 (1992).
  - <sup>28</sup> D. Pogany, S. Bychikhin, M. Litzemberger, E. Gornik, G. Groos, and M. Stecher, *Applied Physics Letters* **81**, 2881 (2002).
  - <sup>29</sup> M. S. Cross and P. C. Hohenberg, *Rev. Mod. Phys.* **65**, 851 (1993).
  - <sup>30</sup> Y. Kuramoto, *Chemical Oscillation, Waves and Turbulence* (Springer-Verlag, Berlin, 1988).
  - <sup>31</sup> A. S. Mikhailov, *Foundations of Synergetics* (Springer-Verlag, Berlin, 1994).
  - <sup>32</sup> *Self-organization in Activator-Inhibitor Systems: Semiconductors, Gas Discharge, and Chemical Active Media*, edited by H. Engel, F.-J. Niedernostheide, H.-G. Purwins, E. Schöll (Wissenschaft&Technik, Berlin, 1996).
  - <sup>33</sup> *Evolution of Spontaneous Structures in Dissipative Continuous Systems*, edited by F. H. Busse and S. C. Müller (Springer, Berlin, 1998).
  - <sup>34</sup> A. Wacker and E. Schöll, *Z. Phys. B: Condens. Matter* **93**, 431 (1994).
  - <sup>35</sup> F.-J. Niedernostheide, H. Schulze, S. Bose, A. Wacker, and E. Schöll, *Phys. Rev. E* **54**, 1253 (1996).
  - <sup>36</sup> S. Bose, P. Rodin, and E. Schöll, *Phys. Rev. E* **62**, 1778 (2000).
  - <sup>37</sup> F. Plenge, P. Rodin, E. Schöll, and K. Krischer, *Phys. Rev. E* **64**, 056229 (2001).
  - <sup>38</sup> K. Penner, *Journal de Physique: Colloque C4* **49**(9), 797 (1988).
  - <sup>39</sup> D. Pogany, S. Bychikhin, E. Gornik, M. Denison, N. Jensen, G. Groos, and M. Stecher, *Proc. IEEE Int. Reliab. Phys. Symp., IRPS2003, Dallas, Texas, 2003*, p.241.
  - <sup>40</sup> G. Wachutka, *IEEE Transactions on Electron Devices* **38**, 1516 (1991).
  - <sup>41</sup> M. Meixner, P. Rodin, E. Schöll and A. Wacker, *Eur. Phys. J. B* **13**, 157 (2000).
  - <sup>42</sup> P. Rodin and E. Schöll, *J. Appl. Phys.* **93**, 6347 (2003).
  - <sup>43</sup> Here we neglect dependence of  $T^*$  and  $T_*$  on  $u$ , assuming  $u = u_{co}$ . This does not change the results.
  - <sup>44</sup> J. Guckenheimer and P. Holmes, *Nonlinear Oscillations, Dynamical Systems, and Bifurcations of Vector Fields*, Vol. 42 of *Applied Mathematical Sciences* (Springer-Verlag, Berlin, 1983).
  - <sup>45</sup> K. Krischer and A. Mikhailov, *Phys. Rev. Lett.* **73**, 3165 (1994).
  - <sup>46</sup> C.P. Schenk, M. Or-Guil, M. Bode and H.-G. Purwins, *Phys. Rev. Lett.* **78**, 3781 (1997).
  - <sup>47</sup> F.-J. Niedernostheide, M. Or-Guil, M. Kleinkes, and H.-G. Purwins, *Phys. Rev. E* **55**, 4107 (1997).
  - <sup>48</sup> H. Hempel, I. Schebesh, and L. Schimansky-Geier, *Eur. Phys. J.* **2**, 399 (1998).
  - <sup>49</sup> M. Or-Guil, M. Bode, C.P. Schenk, and H.-G. Purwins, *Phys. Rev. E* **57**, 6432 (1998).
  - <sup>50</sup> M. Bode, A.W. Liehr, C.P. Schenk, and H.-G. Purwins, *Physica D* **161**, 45 (2002).
  - <sup>51</sup> F. Mertens, R. Imbihl, and A. Mikhailov, *J. Chem. Phys.* **101**, 9903 (1994).
  - <sup>52</sup> M. Falcke and H. Engel, *J. Chem. Phys.* **101**, 6255 (1994).
  - <sup>53</sup> M. Bertram and A. Mikhailov, *Phys. Rev. E* **67**, 036207 (2003).
  - <sup>54</sup> M. Bertram, C. Beta, M. Pollmann, A. Mikhailov, H. Potermund, and G. Ertl, *Phys. Rev. E* **67**, 036208 (2003).
  - <sup>55</sup> A.N. Zaikin and A.M. Zhabotinsky, *Nature* **225**, 535 (1970).
  - <sup>56</sup> E. Mihaliuk, T. Sakurai, F. Chirila, and K. Showalter, *Phys. Rev. E* **65**, 065602(R) (2002).
  - <sup>57</sup> B. Datsko, *Semiconductors* **31**, 146 (1997) [*Fiz. Tekh. Poluprovodn.* **11**, 250 (1996)].

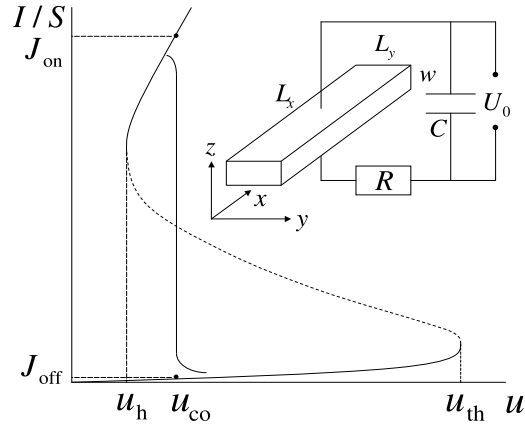


FIG. 1: Current-voltage characteristic of a bistable structure. The average current density  $I/S$  is shown, where  $S = L_x L_y$  is the cross-section of the structure. Unstable middle branch with negative differential conductance is depicted by the dashed line. The hold and threshold voltages are denoted as  $u_h$  and  $u_{th}$ , respectively. The vertical branch at  $u = u_{co}$  corresponds to a static filament. The inset shows a sketch of a bistable semiconductor structure operated in the external circuit with load resistance  $R$ , capacitance  $C$ , and bias  $U_0$ .

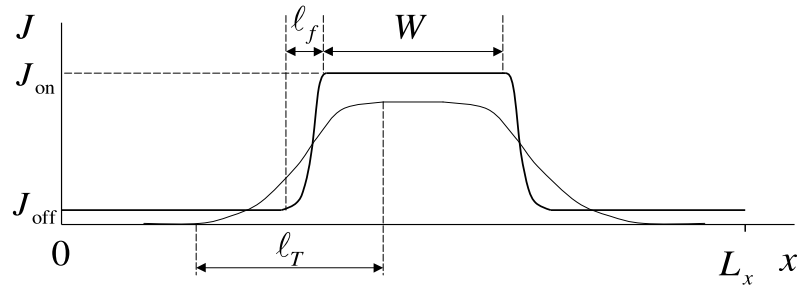


FIG. 2: Current density profile in a filament (thick line). Thin line denotes the temperature profile in the static filament.

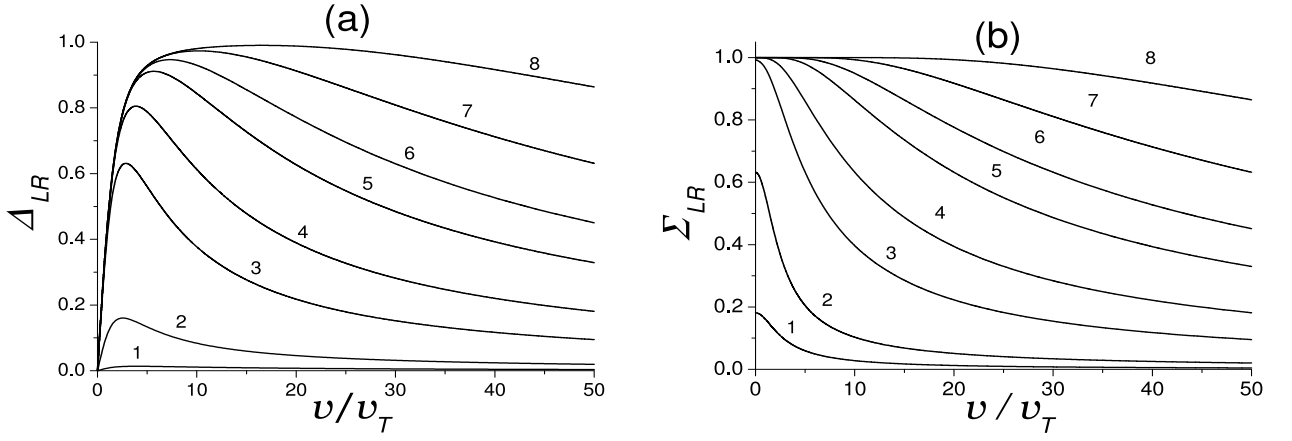


FIG. 3: The normalized difference  $\Delta_{LR}$  (a) and the sum  $\Sigma_{LR}$  (b) of the temperatures in the filament walls  $T_L$  and  $T_R$  as functions of the filament velocity  $v$  for different filament widths  $W$ .  $\Delta_{LR}$  and  $\Sigma_{LR}$  are defined by Eqs. (23), (25), (26). Curves 1 to 8 correspond to  $W/\ell_T = 0.2, 1, 5, 10, 20, 30, 50, 100$ , respectively.

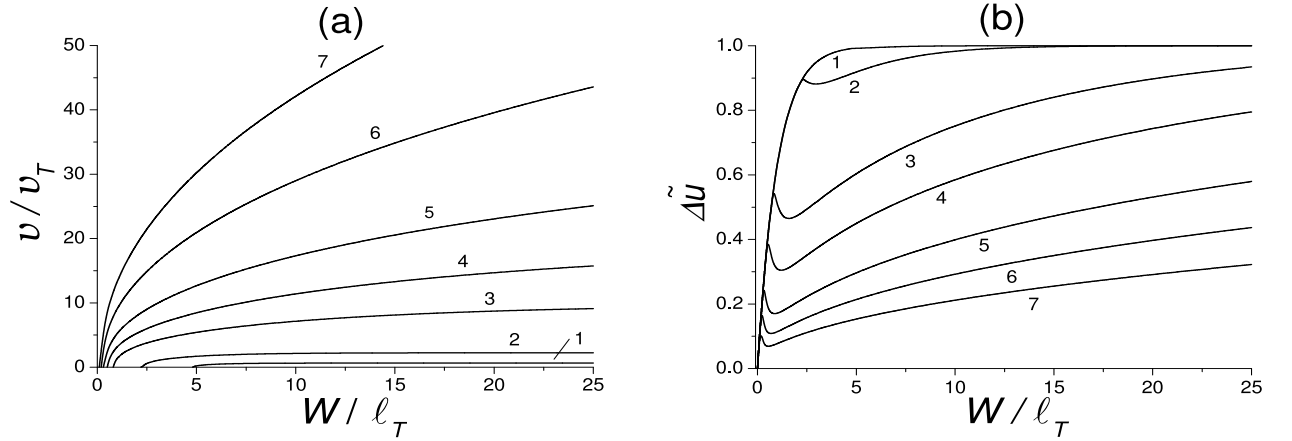


FIG. 4: The filament velocity  $v$  (a) and normalized voltage on the structure  $\Delta \tilde{u}$  (b) as functions of the filament width  $W$  for different values of the parameter  $v_0$ .  $\Delta \tilde{u}$  is defined by Eq. (30). Curves 1 to 7 correspond to  $v_0 = 2.1, 3, 10, 20, 50, 100, 200$ , respectively. Peaks on the voltage curves are related to onset of the filament motion.

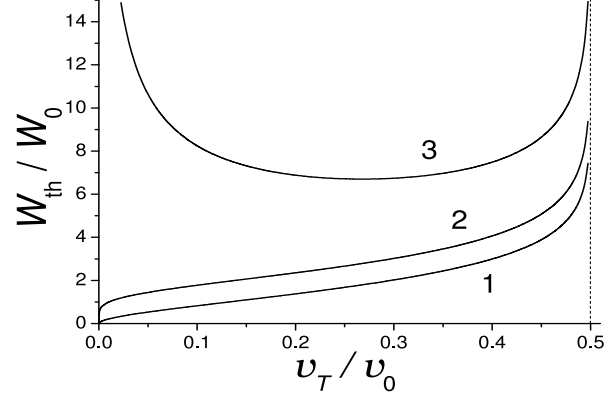


FIG. 5: Normalized threshold filament width  $W_{\text{th}}$  corresponding to onset of the filament motion as a function of  $v_T/v_0$ . Curve 1 shows  $W_{\text{th}}$  normalized to the thermal diffusion length:  $W_0 = \ell_T$ . Curve 2 shows  $W_{\text{th}}$  normalized to the quantity  $W_0 = (D_T^2 \tau_T / v_0)^{1/3}$ , which does not depend on the heat transfer coefficient  $\gamma$ . Curve 3 shows  $W_{\text{th}}$  normalized to the quantity  $W_0 = \sqrt{D_T / v_0}$ , which does not depend on the structure width  $w$ .